Global Biogeochemical Cycles

RESEARCH ARTICLE
10.1029/2020GB006808

Key Points:

- Nonlinear temperature effect on global ocean chlorophyll *a* was found
- Chlorophyll *a* increased with increasing temperatures up to around 14°C
- Chlorophyll *a* decreased with increasing temperatures above 14°C

Supporting Information:

Supporting Information may be found in the online version of this article.

Correspondence to:

J. Feng and N. C. Stenseth,
fengjf@nankai.edu.cn;
n.c.stenseth@ibv.uio.no

Citation:

Feng, J., Stige, L. C., Hessen, D. O., Zuo, Z., Zhu, L., & Stenseth, N. C. (2021). A threshold sea-surface temperature at 14°C for phytoplankton nonlinear responses to ocean warming. *Global Biogeochemical Cycles*, *35*, e2020GB006808. https://doi.org/10.1029/2020GB006808

Received 30 AUG 2020
Accepted 27 APR 2021

A Threshold Sea-Surface Temperature at 14°C for Phytoplankton Nonlinear Responses to Ocean Warming

Jianfeng Feng[1], Leif Chr Stige[2,3], Dag Olav Hessen[2], Zhiling Zuo[1], Lin Zhu[1], and Nils Chr Stenseth[2]

[1]Tianjin Key Laboratory of Environmental Technology for Complex Trans-Media Pollution and Tianjin International Joint Research Center for Environmental Biogeochemical Technology, College of Environmental Science and Engineering, Nankai University, Tianjin, China, [2]Centre of Ecological and Evolutionary Synthesis (CEES), Department of Biosciences, University of Oslo, Oslo, Norway, [3]Norwegian Veterinary Institute, Oslo, Norway

Abstract Marine phytoplankton play a central role in supporting life in the oceans and profoundly affect global biogeochemical cycles. Previous studies have revealed positive effects of sea-surface temperature (SST) on phytoplankton in terms of chlorophyll *a* concentrations (Chla) in high latitude oceans, while negative effects prevail in tropical and midlatitude oceans as well as under stratified summer conditions at higher latitudes. Based on a global analysis of 20 years of ocean Chla and SST data, we first investigated how interannual variability in SST is associated with Chla for each month of the season for every ocean province. We then quantified how the SST-Chla relationships varied with the long-term average (baseline) SST. We found significant season-dependent SST effects on Chla in most ocean provinces. The signs and magnitudes of these effects were consistently associated with the baseline SST, with a shift from positive to negative effects of SST on Chla around 14°C. Based on field observations and literature data, we also estimated the interaction between nitrate limitation and temperature on the SST-Chla relationship. Our findings suggest that the ocean warming effects on Chla depend consistently on the baseline temperature, both with regard to seasonal effects within regions and regional effects between high and low latitude provinces. Our analysis further suggests that the monthly 14°C isotherms can be used as a first approximation to separate areas and seasons where warming has opposite signed effects.

1. Introduction

Marine phytoplankton play a key role in food webs of the oceans as they are responsible for nearly half of the earth's net primary production (Chassot et al., 2010; Field et al., 1998), and have a strong impact on climate as they are major players in the global cycles of nitrogen, phosphorus, and carbon (Beaugrand et al., 2010; Park et al., 2015). Ocean warming will likely impact phytoplankton as temperature affects phytoplankton indirectly via stratification and thus nutrient flux (Cermeño et al., 2008), as well as directly by affecting community composition and metabolic rates (Regaudie-De-Gioux & Duarte, 2012; Thomas et al., 2012). Therefore, predicting the effects of future ocean warming on marine productivity and carbon-sequestration demands a proper understanding of how temperature variation affects phytoplankton production and biomass (Taucher & Oschlies, 2011).

A critical question is whether there are unimodal relations between temperature and marine chlorophyll *a* concentration (Chla), and if thresholds between positive and negative temperature effects can be identified. This is a critical question related to the current warming of surface waters (Cheng et al., 2019; Conroy et al., 2009), with potential abrupt changes in ecosystem processes (Beaugrand et al., 2019). Previous studies have reported negative relationships between sea-surface temperature (SST) and Chla in warm low latitude waters, while positive at high latitudes with annual or seasonal observations (Behrenfeld et al., 2006; Boyce et al., 2010, 2014; Doney, 2006; Irwin & Finkel, 2008; Racault et al., 2012; Roxy et al., 2016). This pattern is also supported by experimental studies (Lewandowska et al., 2014; O'Connor et al., 2009) and models (Hofmann et al., 2011; Taucher & Oschlies, 2011). However, less is known about the strength of the SST-Chla relationship, especially the regional patterns. As SST generally decreases with latitude, we may expect that strengths of the SST-Chla relationships will differ under different temperature regimes, and shift from positive to negative effects as SST exceeds a threshold temperature.

Additionally, several studies on the effect of ocean warming on surface phytoplankton chlorophyll mainly address responses to annual mean temperatures (Behrenfeld et al., 2006; Lewandowska et al., 2014; Llope et al., 2012), which may fail to capture the SST-Chla relationships at finer temporal scales, especially for temperate oceans with large seasonality (Giovannoni & Vergin, 2012). Although previous studies often have failed to detect significant SST-Chla relationships in temperate regions based on annual data, a recent study analyzing monthly data revealed that bell-shaped relationships between SST and Chla were common in the Atlantic and Pacific temperate oceans (Feng et al., 2015).

In this paper, using monthly satellite data from a publicly available database of global chlorophyll concentrations and SST, we test the hypothesis that warming effects on ocean chlorophyll are temperature dependent, i.e., that the sign and strength of SST-Chla relationships depend on baseline temperature, measured as the region-specific and season-specific long-term average SST. Furthermore, the threshold temperature at which temperature effects shifted from positive to negative was quantified. We focus on ocean provinces from 55°S–55°N and 180°W–180°E, which cover the global tropical and temperate oceans (McClain, 2009) (Figure S1). We first investigated how interannual variability in SST is associated with Chla on a monthly basis for every ocean province. Subsequently we quantified how the SST-Chla relationships varied with baseline temperature, and estimated the threshold temperature. Lastly, with data on in situ nitrate concentrations, as well as half-saturation constants for nitrate and experimental growth rate data drawn from literature, the mechanisms involved in this SST-Chla relationship were examined by model analysis.

2. Materials and Methods

2.1. Research Region and Data

Our analysis was based on 30 ocean provinces classified as temperate or tropical oceans (Longhurst, 2010). The names, abbreviations, and locations of each province are listed in Supplementary Table S1 and Figure S1. The southern ocean gyres (SATL, ISSG, and SPSG) were each divided into two subprovinces (SATL1, SATL2, ISSG1, ISSG2, SPSG1, and SPSG2) by the Tropic of Capricorn (23°26′S) in order to compare them with corresponding provinces in the northern oceans (NPSE, NPSW, and NPTG in the North Pacific; NASW, NASE, and NATR in the North Atlantic). The coastal regions (provinces) were excluded from our analysis due to the fact that Chla in these areas is mainly regulated by variations in upwelling and nutrient runoff and is usually orders of magnitude higher than Chla in the open oceans. Further, the remote sensing of Chla in coastal regions is frequently impacted by riverine inputs of dissolved and particulate organic matter.

In our analysis, merged 1° grid level-3 monthly case I ocean time series data on surface chlorophyll *a* concentration (Chla, in mg m^{-3}) from 1998 to 2017 were obtained from the European Space Agency's GlobColour project (Version 2.0) (http://www.globcolour.info/). The merged data sets were created with a Garver, Siegel, and Maritorena (GSM) model and normalized water-leaving radiance observations from the SeaWiFS, MODIS-AQUA, and MERIS ocean color missions (Maritorena & Siegel, 2005). Compared to data from single sensors, the merged products have approximately twice the mean global coverage and lower uncertainties (Maritorena et al., 2010). We also used the weighted average (AVW) Chla product provided by the GlobColour project to do a comparative analysis with GSM Chla. (More information about AVW and GSM derived Chla are provided on http://www.globcolour.info/.) The 1° grid monthly time series SST data from 1998 to 2017 were obtained from the NOAA Extended Reconstructed SST data set (ERSST V3b) (http://www.esrl.noaa.gov/psd/data/gridded).

We are unaware of large-scale spatially resolved time series data on nutrients and mixed layer depth (MLD) that allow exploring the explicit nutrient impact on the SST-Chla associations, thus we here analyze monthly long-term mean MLD and SST data (monthly mean climatologies) to illustrate the SST association with MLD (which subsequently also may affect mixing, nutrients regimes, and thus phytoplankton). The 1° grid monthly mean MLD data were derived from potential temperature and obtained from the NODC (Levitus) World Ocean Atlas (http://www.esrl.noaa.gov/psd/data/gridded/data.nodc.woa94.html). The 1° grid monthly mean SST data for the years 1971–2000 were obtained from the NOAA Optimum Interpolation (OI) Sea-Surface Temperature (SST) Version 2 data set (http://www.esrl.noaa.gov/psd/data/gridded/data.noaa.oisst.v2.html).

2.2. Quantifying the Chla-SST Relationships and Threshold Temperature

To quantify monthly Chla-SST relationships for each ocean province, we first averaged the Chla and SST data per province, year, and month. Then both significant and nonsignificant linear regressions were used to quantify the association between interannual variability in SST and Chla for each month. Original and log-transformed Chla data were both used in this analysis, which provided qualitatively similar results. For comparison, annually averaged data were analyzed similarly.

Season-dependent warming effects on Chla were analyzed using varying-coefficient generalized additive models (vGAMs) (Hastie & Tibshirani, 1990), as implemented in the "mgcv" library in the R environment (Wood, 2006). In this analysis, the monthly resolved SST and Chla data for all 12 months and a given ocean province were analyzed jointly. Chla was modeled as a function of season (month), Chla anomaly of the previous month and temperature anomaly. Chla data were log-transformed. The predictor variables were centered by subtracting the monthly mean values from the observations (annotated by a "Δ" in the variable name). That way, the predictor variables measured the interannual anomalies around the mean seasonal values. The model formula was

$$\log\mathrm{Chla}_{ij} = \mu + f_1\left(\mathrm{Month}_j\right) + f_2\left(\mathrm{Month}_j\right)\cdot\Delta\log\mathrm{Chla}_{i(j\text{-}1)} + f_3\left(\mathrm{Month}_j\right)\cdot\Delta\mathrm{SST}_{ij} + \varepsilon_{ij} \quad (1)$$

Here, $\log\mathrm{Chla}_{ij}$ is ln(Chla) for month j in year i. $\Delta\log\mathrm{Chla}_{i(j-1)}$ is the logChla anomaly for month $j-1$ in year i or year $i-1$ for January, $\Delta\mathrm{SST}_{ij}$ is the SST anomaly for month j in year i. μ is an intercept; f_1, f_2, and f_3 are smooth functions (natural cubic splines) of month (1, 2, ..., 12). f_1 is the month-dependent intercept. f_2 quantifies the month-dependent effect of lagged chlorophyll, which accounts for the possible temporal dependence in the time series. More specifically, this function gives the coefficient for a predictor effect that is linear for any given month but potentially variable in magnitude and sign between months. The function thus shows how the association between the interannual fluctuations in the predictor and response change across the season. The statistical significance of the term refers to a null hypothesis that the coefficient is zero for all months. f_3 is the month-dependent effect function of temperature. ε_{ij} is a normally distributed and independent noise term. To avoid overfitting, the degrees of freedom were restricted to maximum 11 for f_1, which quantifies the mean seasonal pattern for each ocean province, and to maximum 4 for the f_2 and f_3 terms, which explain interannual variability around this mean pattern. Preliminary analyses that allowed more complex shapes of f_2 and f_3 provided functional forms that were complicated to interpret and likely overfitted.

To address the relationship between baseline temperature and strength of SST effects on Chla (warming effects) across the global ocean, we extracted all the coefficients for the SST effect on Chla from significant or nonsignificant linear regression between SST and Chla for every month for each ocean province. These regression slopes, which we here refer to as "warming effect" (mg m^{-3} $°C^{-1}$), were plotted against the monthly baseline SST values. A steeper regression slope with a greater absolute value thus indicates a stronger (positive or negative) warming effect. For ease of interpretation, these analyses were conducted on original-scale Chla data, but we confirmed that results were qualitatively similar using log-transformed data (logChla). A corresponding analysis was also performed on annual scale data.

Regression models were used to quantify the possible relationships between the warming effect (as response variable) and baseline SST (predictor) on a global scale. These relationships were quantified by three methods: Generalized additive models (GAMs), piecewise linear regression ("piecewise LM"), and linear regression ("LM") separately for temperate and for tropical and equatorial ocean provinces For the GAMs, the predictor effect was modeled as a natural cubic spline function with a maximum of 4 degrees of freedom. The threshold temperature (including the 95% confidence intervals), defined as the baseline SST where warming effects on Chla change from positive to negative, was extracted from each of these three models by root finding algorithms. To account for heterogeneity in the uncertainty of the response variable, the inverse of the standard errors of the warming effects was used as weights in these three models.

2.3. Temperature-Dependent Phytoplankton Community Growth Without Nutrient Limitation

Phytoplankton growth rate is directly influenced by temperature (Grimaud et al., 2017). We here estimated the temperature-growth rate relationship using growth rate and temperature data synthesized by Thomas et al. (2012). This global data set includes temperature-limited growth rates of major phytoplankton groups in the ocean, based on >5,000 growth rate measurements for >130 species. The mean growth rates in the data set were estimated for all strains belonging to phytoplankton species between 1980 and 2010. These estimates were based on monthly temperature records at their isolation location and each strain's thermal tolerance curve, and depend on the assumption that growth is limited solely by temperature (Thomas et al., 2012). The influence of temperature on growth rates (g) when nutrients are not limiting growth is commonly described by the Q_{10} model (e.g., Kremer et al., 2017; Sherman et al., 2016) (Equation 2)

$$g\left(T\right) = g_0 \cdot Q_{10}^{\frac{T-T_0}{10}} \left(\mathrm{Q_{10}model}\right) \tag{2}$$

Here, g_0 is the reference growth rate (day^{-1}) at the reference temperature $T_0 = 30°\mathrm{C}$, and the Q_{10} temperature coefficient is a factor of the change in growth rate as a consequence of increasing the temperature, T, by 10°C. These coefficients above were estimated from growth rate and temperature data by the nonlinear least-squares method. Other commonly used functions are the exponential function (Equation 3) and the log-linear function (Equation 4) (Eppley, 1972).

$$g\left(T\right) = \exp\left(K_T T\right) \tag{3}$$

$$\log\left(g\left(T\right)\right) = a \cdot T + b \tag{4}$$

Here, K_T, a, and b are the temperature-dependence coefficients. These functions were simultaneously considered in this study. We determined the best model by comparing their goodness of fit (R^2 and Akaike's Information Criterion) to the observed data (Thomas et al., 2012). The coefficients in Equations 3 and 4 were estimated by the least-squares method.

2.4. Relationship Between Temperature and Nitrate

Nitrate is commonly the key limiting factor for phytoplankton growth rates in the open ocean (Moore et al., 2013) and high temperatures generally coincide with low nitrate concentrations in the upper water layers (Thomas et al., 2017). This is due to the stratification of the water column induced by temperature, which prevents the resuspension of nutrients from deeper waters and sediments after nutrients have been depleted. We here quantified the association between temperature and concentrations of nitrate using data from the uniformly calibrated open ocean data set, containing temperature and nutrient variables (www.glodap.info/index.php/merged-and-adjusted-data-product/). The data sets used in this study generally cover the global ocean (38°S–50°N, 180°W–180°E) and were recorded from 1972 to 2012. In addition, we removed some abnormal data, such as high nitrate values with high temperature in coastal areas. An exponential function was used because of better fit to the observed data than a linear model

$$N = f\left(T\right) = \exp\left(mT\right) \tag{5}$$

Here, N is the concentration of nitrate and m is the temperature-dependent coefficient estimated by the least-squares method.

2.5. Combined Direct and Indirect Effects of Temperature on Phytoplankton

Phytoplankton growth is driven by temperature and nutrients (under sufficient light conditions), and the nutrient limitation could be accentuated by high temperature and increased thermal stability (Thomas et al., 2017). We thus incorporated a functional nutrient (nitrogen) response in terms of a functional response, represented by Michaelis-Menten kinetics, $N/(N + Ks(N))$ (e.g., Marinov et al., 2010), N is the nitrate concentration and $Ks(N)$ is the half-saturation constant. Equations 2–4 and 5 were combined as a joint

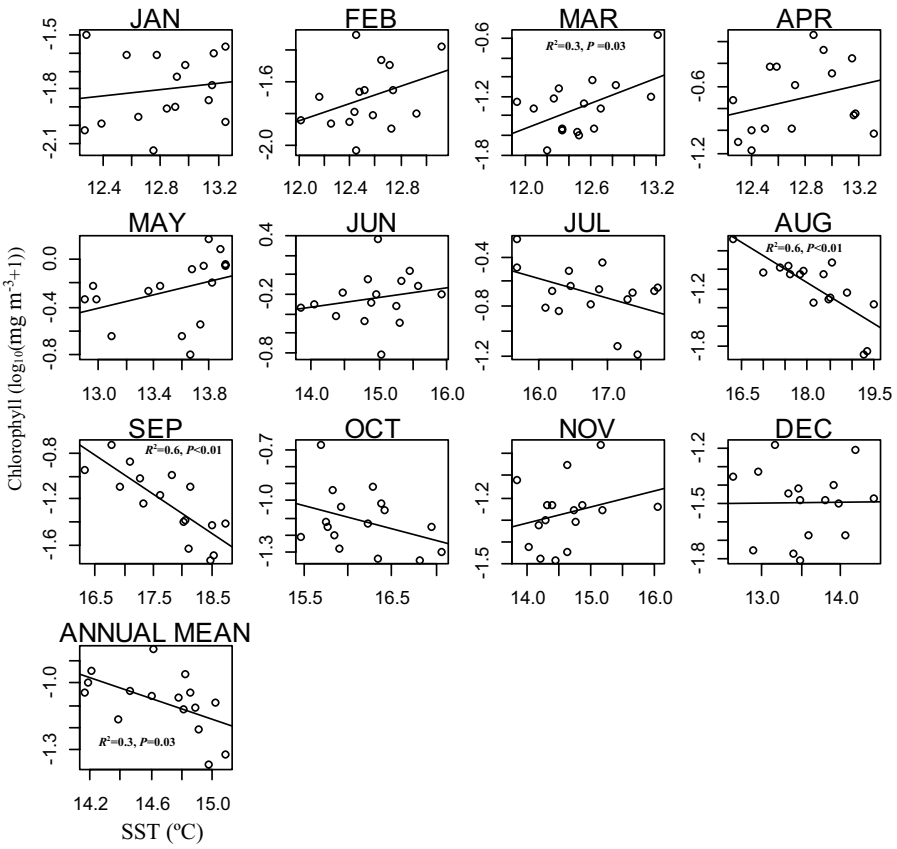

Figure 1. Relationships between sea-surface temperature (SST) and ocean chlorophyll concentrations (log-transformed) with mean monthly and annual data from the North Atlantic Drift (NADR) province. Black lines represent linear regression relationships. The proportions of variance explained (R^2) and p-values are shown for significant relationships ($p < 0.05$).

function of direct and indirect effects of temperature on the growth rate (Marinov et al., 2010; Thomas et al., 2017), which is listed below

$$\mu(T) = g(T)\frac{f(T)}{f(T) + Ks(N)} \tag{6}$$

Here, $\mu(T)$ is the growth rate driven by the temperature and nitrate, the function $f(T)$ is the same as Equation 5, the function of $g(T)$ was the best model of Equations 2–4 that was determined by their goodness of fit to the observed data. $Ks(N)$ is the half-saturation constant obtained from 26 marine phytoplankton species from eight previous studies (Table S2), the mean of which used in the model was calculated by bootstrap method from these phytoplankton species.

3. Results

The analysis revealed different SST-Chla relationships in different months. For example, in the temperate North Atlantic Drift (NADR) region in the Northeast Atlantic, logChla and SST are significantly positively correlated in March ($p < 0.05$), under relatively low temperatures (12.5 ± 0.5°C) (Figure 1), while negative relationships were found in August and September ($p < 0.05$), with relatively high temperatures (17.5 ± 1.5°C). While contrasting SST-Chla relationships were found in warm and cold seasons, the annual logChla and SST data revealed an overall significant negative relationship in this ocean region (Figure 1). Linear regression analysis of SST and logChla in other ocean provinces provided similar results, with often

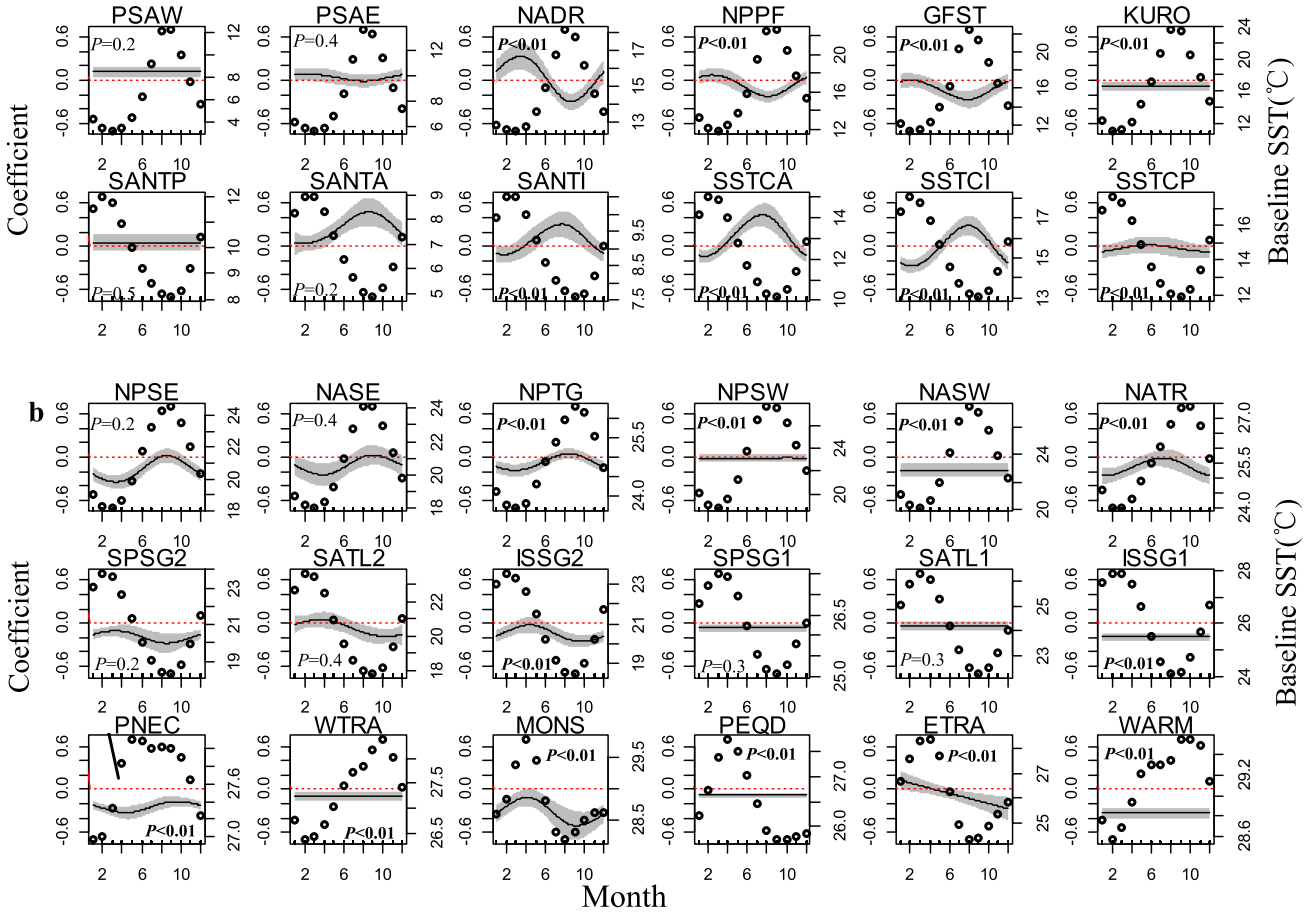

Figure 2. The seasonally variable coefficient for the linear effect of temperature on phytoplankton chlorophyll in temperate oceans (a) and tropical oceans (b). Each panel represents one ocean province (see details in Figure S2). The black lines with gray shading represent the seasonally variable coefficient with 95% confidence intervals. The seasonally variable coefficient represents how much logChla is expected to deviate from the long-term mean for that month for a 1°C anomaly in SST in that month. Temperature effects are significantly different from zero for months for which the confidence intervals do not overlap with the red, dotted zero-effect lines. Baseline SST (right axis, average monthly SST) are plotted with points and broken lines.

contrasting SST-Chla relationships in different seasons (Figure S2). Note that the *p*-values for individual provinces and months should be interpreted with caution due to the large number of tests involved. Across all tests, 113 among 390 *p*-values were <0.05, which is four times higher than the expected number to arise just by chance.

We then used seasonal VGAMs (Hastie & Tibshirani, 1990) to test if there were significant seasonally varying SST-Chl relationships for the 30 ocean provinces, and found significant season-dependent SST effects in 24 of the 30 ocean provinces (Figure 2 and Table S3). In temperate ocean provinces, positive relationships (denoted by a positive coefficient) were generally found in the cold season, while negative relationships were found in the warm season (Figure 2a). In contrast, consistently negative relations were generally found in tropical oceans (Figure 2b).

Both the monthly and annual SST-Chla regression analyses showed that the warming effect on Chla tended to be positive at low baseline temperatures and negative at relatively high baseline temperatures (points in Figure 3). The magnitude of the warming effect estimated by monthly data (Figures 3a–3c) decreased with a rate about -0.006 ± 0.001 mg m^{-3} °C^{-1}°C^{-1} (Table S4). Here, the rate means the slope of the regression models showing how warming effects vary with baseline SST. The magnitude of the warming effect estimated by annual scale analysis displayed a similar pattern (Figures 3e–3g). The conclusion that the SST effects depend on baseline temperature (Figure 3) was also supported by analyses where the strengths of SST-Chla

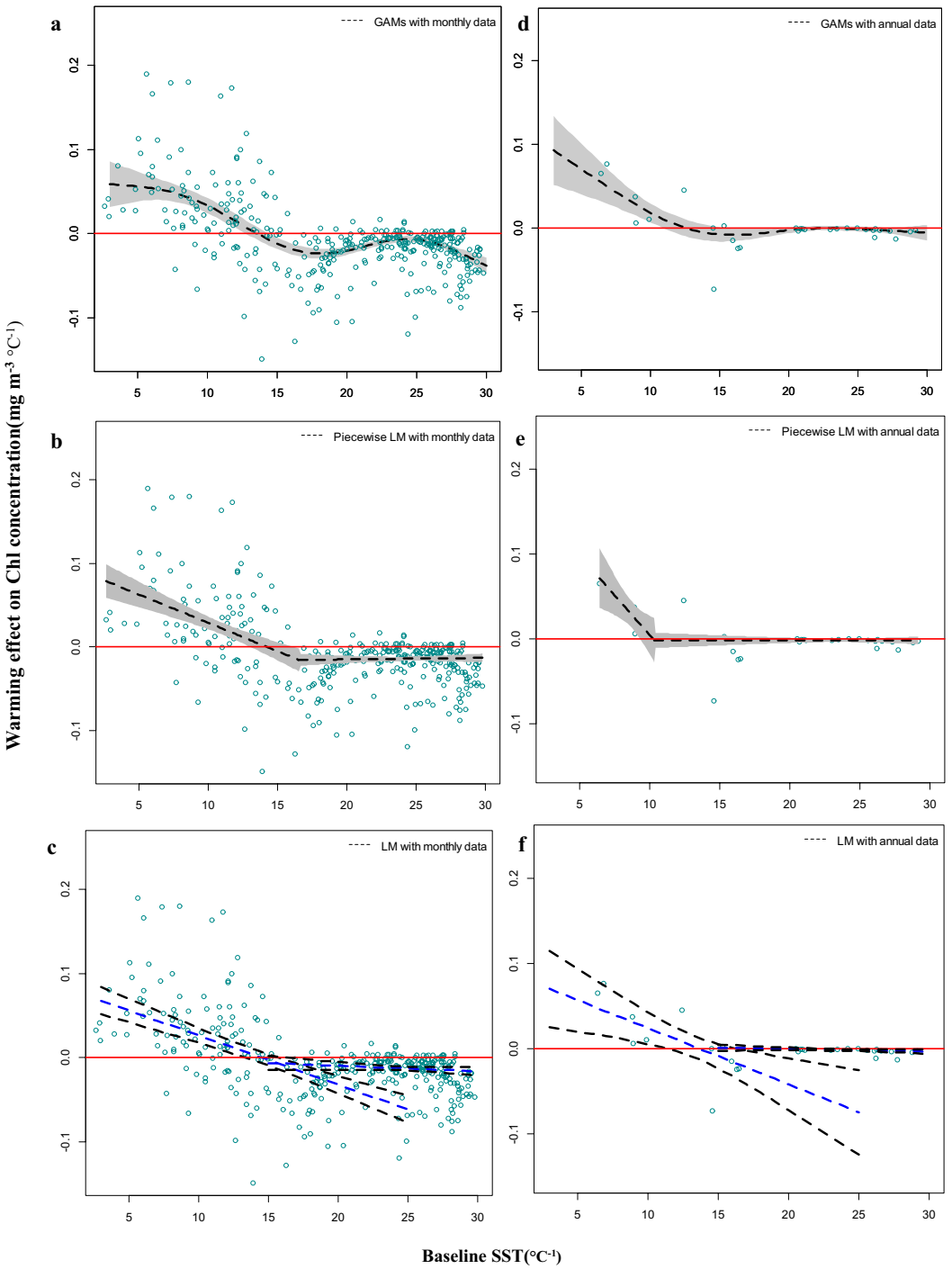

Figure 3. Decreasing warming effect on chlorophyll concentrations with increasing baseline sea-surface temperature. Each point represents the estimated warming effect, i.e., the slope of a linear regression between interannual variability in SST and Chla, in an ocean province for one calendar month (a)–(c) or for the whole year (d)–(f). Three different regression models describe the effect of baseline (i.e., long-term average) SST on the estimated warming effect. Nonlinear effect estimated with GAM ($p < 0.001$) (a, d, dotted black line, with gray shading representing 95% CI). Piecewise linear effect estimated using a segmented function ($p < 0.001$) (b, e, dotted black line, with gray shading representing 95% CI). Linear relationships estimated separately for temperate and tropical and equatorial ocean provinces (c, f, dotted blue lines, with dotted black lines representing 95% CI). Model results are listed in Table S3. Threshold temperatures identified with monthly data were (a) 13.6 ± 0.7°C; (b) 14.3 ± 0.5°C; (c) 14.6 ± 0.6°C, with annual data, (d) 14.0 ± 0.7°C; (e) 14.3 ± 1.3°C; (f) 13.7 ± 1.1°C. More details are presented in Table S5.

relationships were calculated as Pearson correlation coefficients (Figure S3), and where an alternative Chla data set was used (where data from different satellites were merged using AVW instead of GSM model as in the main analysis) (Figure S4).

GAM analyses for all ocean provinces combined suggested that the threshold temperature was near 14°C (13.6 ± 0.7°C for monthly data, Figure 3a and Table S5). Both piecewise linear and linear regression analysis quantified similar threshold temperatures (14.3 ± 0.5°C, Figure 3b and 14.6 ± 0.6°C, Figure 3c). For the annual data, the threshold temperatures estimated by all three models were also nearly 14°C (14.0 ± 0.7°C, Figure 3d; 14.3 ± 1.3°C, Figure 3e; 13.4 ± 1.1°C, Figure 3f), which were slightly lower than the value estimated by seasonal data (Table S5).

The mechanisms involved in the above SST-Chla relationship were supported by model analysis with independent field and experimental growth rate data. We investigated the direct effect of SST on phytoplankton growth rate using solely temperature-limited phytoplankton growth rates data from the Thomas et al. database (Thomas et al., 2012). As expected, a generally positive relationship was found between SST and phytoplankton growth rate under nonnutrient-limited conditions (Figure 4a). The Q_{10} model showed a better fit to the observed data with the $Q_{10} = 1.592$ and $g_0 = 1.0625$ (day^{-1}) than the other two models (Q_{10} model: $R^2 = 0.382$; exponential function: $R^2 = 0.145$; linear function: $R^2 = 0.158$; Figure S5). For the indirect effect of SST on phytoplankton, we found a negative relationship between the nitrate concentration and SST (Figure 4b). This negative relationship was better described by an exponentially decreasing function with $c = 38.73$, $m = -0.16$ (Figure 4b) than by a log-linear model. Last, combining the direct and indirect effects of SST on the phytoplankton community growth rate together (Equation 6 in Section 2), we found that the growth-temperature relationship is a distinctive threshold temperature above which increasing SST has negative effect on growth rate under nutrient limitation (red lines in Figure 4c). This pattern is true not only for different regions but also for different seasons. The histogram of the estimated threshold temperature values considering the variability of half-saturation constants ($Ks(N)$ in Table S2) and the parameters in Equations 2 and 5 (Table S6) is shown in Figure 4d. The threshold temperature values were quantified at 14.1 ± 6.9°C (Figure 4d).

4. Discussion

By analyzing 20 years of ocean chlorophyll concentration and sea-surface temperature data, we estimated the strengths of the SST-Chla relationships under different temperature regimes, and quantified the threshold temperature at which the temperature effects shift form positive to negative. Our analyses confirm other studies suggesting that future climate warming will decrease phytoplankton chlorophyll in surface waters in the typically nutrient-limited tropical regions (low latitude and midlatitude), while promoting phytoplankton chlorophyll at higher latitudes (Chust et al., 2014). Furthermore, we found that the warming effects on chlorophyll concentration were more positive in areas, and seasons, where sea-surface temperatures generally were lower (Figure 3). Specifically, with increasing SST from 3 to 30°C, the magnitude of the warming effect decreased from 0.08 ± 0.02 mg m^{-3} $°C^{-1}$ at the lowest temperatures to a minimum of −0.02 ± 0.015 mg m^{-3} $°C^{-1}$at around 16°C with a rate of about −0.007 ± 0.001 mg m^{-3} $°C^{-1}$$°C^{-1}$, and then remained constant at −0.02 ± 0.005 mg m^{-3} $°C^{-1}$ above that temperature. A corresponding regional pattern has been described in other studies (Behrenfeld et al., 2006; Boyce et al., 2010; Feng et al., 2015), but to our knowledge, not quantitatively linked to the pattern in baseline temperature as well as to seasonal changes in temperature effects.

This spatial-temporal pattern in the SST-Chla relationship could be due to a combination of direct physiological impacts (e.g., the ratio of respiration to C-fixation increases with temperature, reducing net C-acquisition) and indirect effects related to nutrient scarcity with shallower mixing depth. Meta-analysis of various phytoplankton groups over a wide latitudinal gradient has shown that the optimum temperature for growth generally exceeds the mean ambient temperature by several degrees (Thomas et al., 2012). This implies that an above-average temperature (of up to around +5°C compared to the local mean) will always promote phytoplankton growth given that other factors such as light and nutrients are not limiting. However, ocean warming could also increase water column stability, which will inhibit vertical mixing and consequently the supply of nutrients to the mixed layer (Dave & Lozier, 2013). Monthly MLD and SST

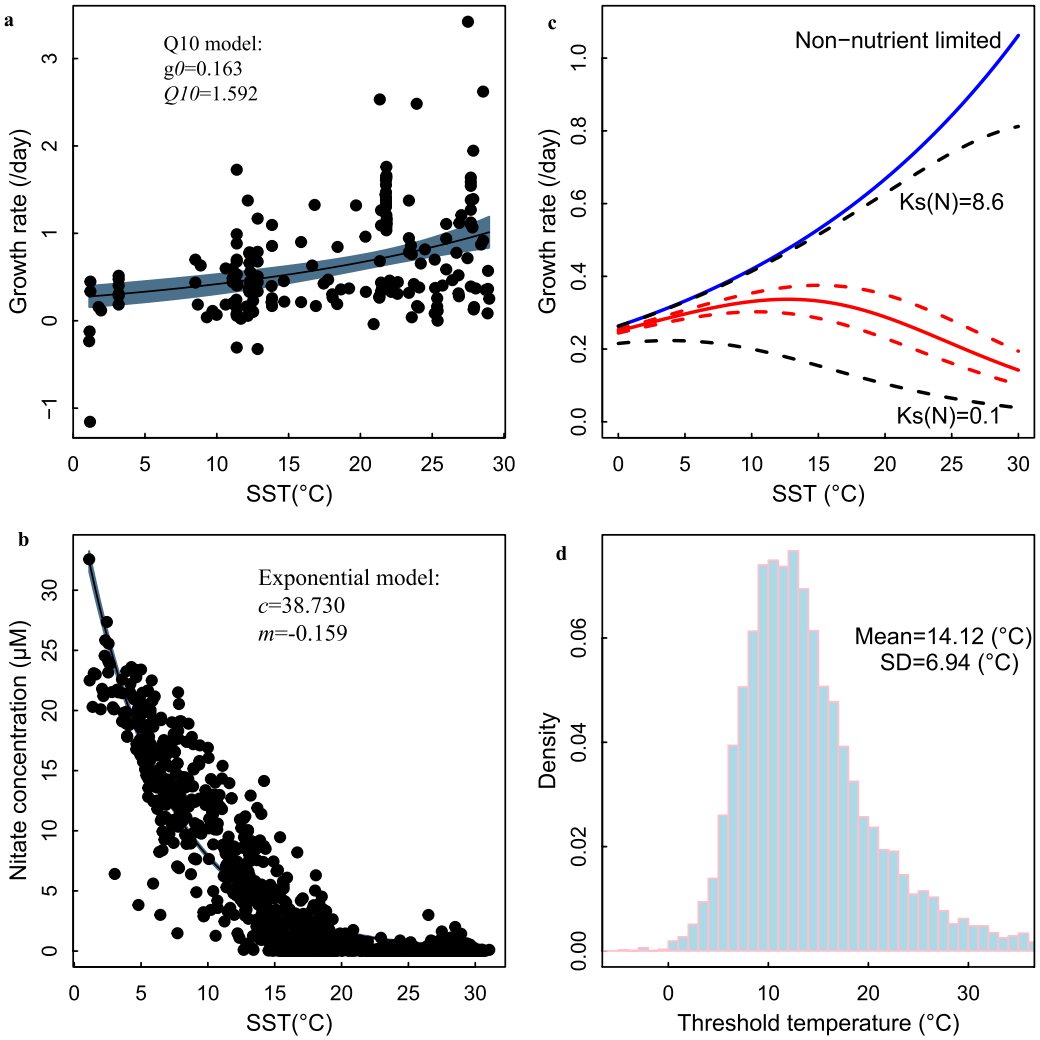

Figure 4. The relationship between temperature and phytoplankton community growth rate. (a) Observed phytoplankton community growth rate across a gradient of ocean temperature. The blue line is the regression line with 95% confidence intervals (blue region). The regression line shown is for the best model, which displays the growth-temperature relationship with the best fit to the Q_{10} model ($R^2 = 0.38$, $p < 0.0001$). (b) Observed nitrate concentration is plotted vs. sea-surface temperature. The blue line and 95% confidence bands (blue) display the modeled nitrate-temperature relationship with the best fit to the exponential model ($R^2 = 0.86$, $p < 0.0001$). (c) Phytoplankton community growth rate with and without nitrate limitation is plotted vs. the temperature. The blue line shown is the growth-temperature relation modeled by Q_{10} equation without nitrate limitation. The solid red line with dotted lines representing 95% CI display the effect of temperature on the growth with nitrate limitation under the average value of *Ks*(*N*). The black dotted lines represent the effect of temperature on the growth with the maximum *Ks*(*N*) (8.6) and minimum *Ks*(*N*) (0.1), respectively. (d) Histogram of the estimated threshold temperature values considering the uncertainty of the parameters in Equations 2 and 5 and Table S2.

clearly showed that MLD generally decreased with elevated SST (Figures S7 and S8), supporting that nutrient limitation and photoacclimation could be the ultimate cause of the negative temperature effects on phytoplankton chlorophyll in warm areas.

The abovementioned mechanism involved in this SST-Chla relationship was also clearly supported by the regression and GAM analysis with independent field and experimental data. Temperature exerts a large effect on the phytoplankton community growth rates (Eppley, 1972; Thomas et al., 2017). The direct effect of SST on the phytoplankton community growth rate generally shows an exponential positive relationship (Sherman et al., 2016; Thomas et al., 2012) as shown in Figure 4a. Nitrate concentration also plays a

significant role in the phytoplankton growth rates (Moore et al., 2013). We represented the indirect effect of SST through a temperature effect on nutrient limitation. Nitrate concentration exponentially declines with increasing temperature and maintains a low level when approximately above 15°C (Figure 4b). Marinov et al. (2010) proposed the existence of a critical nutrient threshold corresponding to 45°S and 45°N in the open sea. In the 45°S–45°N region (tropical and equatorial ocean provinces), high temperature leads to low nitrate concentration due to temperature-induced stratification of the water column (Marinov et al., 2010). The combined effects of SST and nitrate limitation induced by high temperature are modeled with a multiplicative term (Equation 6). The results indicated that the phytoplankton growth rates begin to decline at around 14°C under the combined effect (Figure 4c), which is consistent with the observed satellite data analysis.

The threshold effect of temperature on chlorophyll *a* was affected by the half-saturation constant *Ks*(*N*) (Figure 4c, Figure S6). We noticed that the standard deviation of the threshold temperature is about 7°C (Figure 4d), which suggested that the range of possible threshold temperature values where nitrogen limitation causes growth rates to decline is broad [7.18°C, 21.06°C]. This variability in threshold temperature likely reflects differences in phytoplankton community composition, as well as their physiological status. While latitudinal patterns in the thermal traits of phytoplankton have been observed (Chakraborty et al., 2020; Thomas et al., 2012), far less is known about the distribution of *Ks*(*N*) values within communities and across latitudes. For example, small phytoplankton with lower *Ks*(*N*) are influenced strongly by nutrient limitation in high temperature conditions, whereas diatoms with higher *Ks*(*N*) are also limited by nutrients in low temperature conditions. Our analysis was based on the mean of half-saturation constants *Ks*(*N*) for 26 disparate marine species (Table S2), which is only a small portion of the species included in the growth rate vs. temperature analysis (Figure 4a). While the predictions should be read with some caution due to the variability of *Ks*(*N*) across species and communities, the detected threshold in chlorophyll *a* to temperature (e.g., Figure 3) may arise due to an intensification of nitrogen limitation, supported by our modeling work with the threshold temperature value about 14°C.

These analyses suggest that a possible net balance between positive and negative effects was reached at around 14°C, which is consistent with observed unimodal temperature responses in many temperate ocean provinces (Feng et al., 2015). Similarly, Behrenfeld et al. (2006) suggested a threshold of annual mean SST of around 15°C separating permanently stratified tropical regions with predominantly negative SST-Chla associations from temperate regions with indications of positive associations. By showing that such a global pattern is statistically significant when data for additional years are available and that it extends to seasonal changes in SST-Chla associations, we can have increased confidence in the robustness of the association.

Many studies addressing potential effects of climate change on ocean phytoplankton have been performed on an annual basis (Chavez et al., 2011; Lewandowska et al., 2014), which may fail to detect biologically important season-dependent responses (Boersma et al., 2016). Interestingly, we found that the global pattern in the association between baseline SST and the sign and strength of warming effects on Chla is reproduced at a seasonal scale (Figure 3). For regions with large seasonality in temperature, it follows that warming is likely to influence chlorophyll *a* differently in different seasons. For example, for NADR (Figure S2) we found that a relatively weak negative Chla-SST association at an annual scale was caused by strongly negative associations in summer, which were partly, but not fully, compensated by positive associations in winter. Significant season-dependent SST effects were detected in 24 of the 30 ocean provinces (Figure 2), suggesting globally wide-spread SST effects on phytoplankton phenology. For food-web dynamics, these seasonal changes may be more important than the interannual fluctuations.

Chlorophyll *a* concentration is the most wide-spread proxy for estimating large-scale phytoplankton biomass patterns through remote sensing (Kahru et al., 2014; Moses et al., 2009; Sipelgas et al., 2006). Chla:C-ratio of phytoplankton may, however, be modified by variables such as nutrient concentration and light level (Behrenfeld et al., 2016; Toseland et al., 2013). Thus, increased light exposure and spectral changes related to optical properties in the water column could affect photoacclimation and mass-specific chlorophyll (Falkowski & LaRoche, 1991). SST may also, as discussed above, covary with nutrient concentration through associations with stratification and mixing regimes. Adding to this, there will also be some variations in Chla:C-ratio related to phytoplankton community composition (Geider & La Roche, 2002), which may vary both spatially, seasonally, and also interannually (Alvain et al., 2008; Dandonneau et al., 2004).

Species adapted to fluctuating light environments seem to have narrower ranges of Chla:C compared to species adapted to more stable light environments (Talmy et al., 2013). More work is needed to fully account for the effects of varied nutrient stoichiometry and photoacclimation on the relationship between C and Chla (or other biomass proxies). Despite these potential modifications, Chla is a widely used and good proxy of phytoplankton biomass in open waters, and directly related to photosynthesis (Boyce et al., 2010).

Nevertheless, we acknowledge some limitations of our study. First, SST has a positive effect on microzooplankton grazing rate and indirectly influences the phytoplankton growth rate (Sherman et al., 2016), which was not considered in the model analysis. In addition, light and iron are also important factors limiting growth in phytoplankton (Edwards et al., 2016; Moore et al., 2013). Dispersal may also affect community composition and may reflect both current conditions and species sorting due to historical exposure to abiotic conditions (Doblin & van Sebille, 2016). Finally, one important covariate to consider when studying temperature effects is cell size (Kremer et al., 2017), which affects both growth rate and nutrient uptake. Communities composed of large vs. small cells will likely possess differences in $Ks(N)$ and then also affect the estimated threshold temperature. Understanding the combined effect of multiple factors on phytoplankton growth is a challenging goal that is nevertheless necessary in order to accurately forecast the phytoplankton dynamics under ocean warming expectations.

5. Conclusions

By analyzing 20 years of ocean chlorophyll *a* concentration and SST data with GAM, we found that signs and magnitudes of warming effects on Chla were consistently associated with the region-specific and season-specific long-term average temperature. The results showed that a shift between positive and negative effects of temperature on Chla was found around 14°C. These findings suggest that the ocean warming effects on Chla are consistently associated with baseline temperature, both with regard to seasonal effects within regions and regional effects between high and low latitude provinces. We do not claim a universal threshold at 14°C, clearly this will depend on phytoplankton community composition, nutrient regimes and nutrient regeneration, thermal stratification, and other factors. Still a temperature threshold around the 14°C isotherms is in support of previous studies, and can be used as a first approximation to separate areas and seasons where warming has opposite signed effects. Our findings also provide a new method to explain complex, nonlinear temperature effects: As global warming continues, we expect that the areas and months with temperatures <14°C, in which warming appears to be positive for ocean Chla, will decrease.

Data Availability Statement

We thank the GlobColour project, NASA Ocean Color Processing Group and NOAA NODC for satellite data provided at their website (http://www.globcolour.info/; http://www.esrl.noaa.gov/psd/data/gridded; http://www.esrl.noaa.gov/psd/data/gridded/data.nodc.woa94.html). We also thank Bjerknes Climate Data Centre and the ICOS Ocean Thematic Centre who hosted the GLODAP website (https://www.glodap.info/).

Acknowledgments
This work was supported by the National Key R&D Program of China (2018YFC1406403) and the Nordforsk-funded GreenMAR project.

References

Alvain, S., Moulin, C., Dandonneau, Y., & Loisel, H. (2008). Seasonal distribution and succession of dominant phytoplankton groups in the global ocean: A satellite view. *Global Biogeochemical Cycles*, *22*, GB3001. https://doi.org/10.1029/2007GB003154

Beaugrand, G., Conversi, A., Atkinson, A., Cloern, J., Chiba, S., Fonda-Umani, S., et al. (2019). Prediction of unprecedented biological shifts in the global ocean. *Nature Climate Change*, *9*, 237–243. https://doi.org/10.1038/s41558-019-0420-1

Beaugrand, G., Edwards, M., & Legendre, L. (2010). Marine biodiversity, ecosystem functioning, and carbon cycles. *Proceedings of the National Academy of Sciences of the United States of America*, *107*(22), 10120–10124. https://doi.org/10.1073/pnas.0913855107

Behrenfeld, M. J., O'Malley, R. T., Boss, E. S., Westberry, T. K., Graff, J. R., Halsey, K. H., et al. (2016). Revaluating ocean warming impacts on global phytoplankton. *Nature Climate Change*, *6*(3), 323–330. https://doi.org/10.1038/nclimate2838

Behrenfeld, M. J., O'Malley, R. T., Siegel, D. A., McClain, C. R., Sarmiento, J. L., Feldman, G. C., et al. (2006). Climate-driven trends in contemporary ocean productivity. *Nature*, *444*, 752–755. https://doi.org/10.1038/nature05317

Boersma, M., Gruner, N., Signorelli, N. T., Gonzalez, P. E. M., Peck, M. A., & Wiltshire, K. H. (2016). Projecting effects of climate change on marine systems: Is the mean all that matters? *Proceedings of the Royal Society B: Biological Sciences*, *283*(1823), 20152274. https://doi.org/10.1098/rspb.2015.2274

Boyce, D. G., Dowd, M., Lewis, M. R., & Worm, B. (2014). Estimating global chlorophyll changes over the past century. *Progress in Oceanography*, *122*, 163–173. https://doi.org/10.1016/j.pocean.2014.01.004

Boyce, D. G., Lewis, M. R., & Worm, B. (2010). Global phytoplankton decline over the past century. *Nature*, *466*(7306), 591–596. https://doi.org/10.1038/nature09268

Cermeño, P., Dutkiewicz, S., Harris, R. P., Follows, M., Schofield, O., & Falkowski, P. G. (2008). The role of nutricline depth in regulating the ocean carbon cycle. *Proceedings of the National Academy of Sciences of the United States of America*, *105*(51), 20344–20349. https://doi.org/10.1073/pnas.0811302106

Chakraborty, S., Cadier, M., Visser, A. W., Bruggeman, J., & Andersen, K. H. (2020). Latitudinal variation in plankton traits and ecosystem function. *Global Biogeochemical Cycles*, *34*, e2020GB006564. https://doi.org/10.1029/2020GB006564

Chassot, E., Bonhommeau, S., Dulvy, N. K., Mélin, F., Watson, R., Gascuel, D., & Le Pape, O. (2010). Global marine primary production constrains fisheries catches. *Ecology Letters*, *13*(4), 495–505. https://doi.org/10.1111/j.1461-0248.2010.01443.x

Chavez, F. P., Messie, M., & Pennington, J. T. (2011). Marine primary production in relation to climate variability and change. *Annual Review of Marine Science*, *3*(3), 227–260. https://doi.org/10.1146/annurev.marine.010908.163917

Cheng, L., Abraham, J., Hausfather, Z., & Trenberth, K. E. (2019). How fast are the oceans warming? *Science*, *363*(6423), 128–129. https://doi.org/10.1126/science.aav7619

Chust, G., Allen, J. I., Bopp, L., Schrum, C., Holt, J., Tsiaras, K., et al. (2014). Biomass changes and trophic amplification of plankton in a warmer ocean. *Global Change Biology*, *20*(7), 2124–2139. https://doi.org/10.1111/gcb.12562

Conroy, J., Restrepo, A., Overpeck, J., Steinitz-Kannan, M., Cole, J. E., Bush, M. B., & Colinvaux, P. A. (2009). Unprecedented recent warming of surface temperatures in the eastern tropical Pacific Ocean. *Nature Geoscience*, *2*, 46–50. https://doi.org/10.1038/ngeo390

Dandonneau, Y., Deschamps, P. Y., Nicolas, J. M., Loisel, H., Blanchot, J., Montel, Y., et al. (2004). Seasonal and interannual variability of ocean color and composition of phytoplankton communities in the North Atlantic, equatorial Pacific and South Pacific. *Deep-Sea Research Part II-Topical Studies in Oceanography*, *51*(1–3), 303–318. https://doi.org/10.1016/j.dsr2.2003.07.018

Dave, A. C., & Lozier, M. S. (2013). Examining the global record of interannual variability in stratification and marine productivity in the low-latitude and mid-latitude ocean. *Journal of Geophysical Research: Oceans*, *118*, 3114–3127. https://doi.org/10.1002/jgrc.20224

Doblin, M. A., & van Sebille, E. (2016). Drift in ocean currents impacts intergenerational microbial exposure to temperature. *Proceedings of the National Academy of Sciences of the United States of America*, *113*(20), 5700–5705. https://doi.org/10.1073/pnas.1521093113

Doney, S. C. (2006). Plankton in a warmer world. *Nature*, *444*, 695–696. https://doi.org/10.1038/444695a

Edwards, K. F., Thomas, M. K., Klausmeier, C. A., & Litchman, E. (2016). Phytoplankton growth and the interaction of light and temperature: A synthesis at the species and community level. *Limnology and Oceanography*, *61*(4), 1232–1244. https://doi.org/10.1002/lno.10282

Eppley, R. W. (1972). Temperature and phytoplankton growth in the sea. *Fishery Bulletin*, *70*(4), 1063–1085.

Falkowski, P. G., & LaRoche, J. (1991). Acclimation to spectral irradiance in algae. *Journal of Phycology*, *27*(1), 8–14. https://doi.org/10.1111/j.0022-3646.1991.00008.x

Feng, J., Durant, J. M., Stige, L. C., Hessen, D. O., Hjermann, D. Ø., Zhu, L., et al. (2015). Contrasting correlation patterns between environmental factors and chlorophyll levels in the global ocean. *Global Biogeochemical Cycles*, *29*, 2095–2107. https://doi.org/10.1002/2015GB005216

Field, C. B., Behrenfeld, M. J., Randerson, J. T., & Falkowski, P. (1998). Primary production of the biosphere: Integrating terrestrial and oceanic components. *Science*, *281*(5374), 237–240. https://doi.org/10.1126/science.281.5374.237

Geider, R., & La Roche, J. (2002). Redfield revisited: Variability of C:N:P in marine microalgae and its biochemical basis. *European Journal of Phycology*, *37*(1), 1–17. https://doi.org/10.1017/s0967026201003456

Giovannoni, S. J., & Vergin, K. L. (2012). Seasonality in ocean microbial communities. *Science*, *335*(6069), 671–676. https://doi.org/10.1126/science.1198078

Grimaud, G. M., Mairet, F., Sciandra, O., & Bernard, O. (2017). Modeling the temperature effect on the specific growth rate of phytoplankton: A review. *Reviews in Environmental Science and Biotechnology*, *16*(4), 625–645. https://doi.org/10.1007/s11157-017-9443-0

Hastie, T., & Tibshirani, R. (1990). Generalized additive models. In Monographs on statistics and applied probability (Vol. 43). London: Chapman & Hall.

Hofmann, M., Worm, B., Rahmstorf, S., & Schellnhuber, H. J. (2011). Declining ocean chlorophyll under unabated anthropogenic CO_2 emissions. *Environmental Research Letters*, *6*(3), 034035. https://doi.org/10.1088/1748-9326/6/3/034035

Irwin, A. J., & Finkel, Z. V. (2008). Mining a sea of data: Deducing the environmental controls of ocean chlorophyll. *PLoS ONE*, *3*(11), e3836. https://doi.org/10.1371/journal.pone.0003836

Kahru, M., Kudela, R., Anderson, C., Manzano-Sarabia, M., & Mitchell, B. (2014). Evaluation of satellite retrievals of ocean chlorophyll-a in the California Current. *Remote Sensing*, *6*(9), 8524–8540. https://doi.org/10.3390/rs6098524

Kremer, C. T., Thomas, M. K., & Litchman, E. (2017). Temperature- and size-scaling of phytoplankton population growth rates: Reconciling the Eppley curve and the metabolic theory of ecology. *Limnology and Oceanography*, *62*, 1658–1670. https://doi.org/10.1002/lno.10523

Lewandowska, A. M., Boyce, D. G., Hofmann, M., Matthiessen, B., Sommer, U., & Worm, B. (2014). Effects of sea surface warming on marine plankton. *Ecology Letters*, *17*(5), 614–623. https://doi.org/10.1111/ele.12265

Llope, M., Licandro, P., Chan, K.-S., & Stenseth, N. C. (2012). Spatial variability of the plankton trophic interaction in the North Sea: A new feature after the early 1970s. *Global Change Biology*, *18*(1), 106–117. https://doi.org/10.1111/j.1365-2486.2011.02492.x

Longhurst, A. R. (2010). *Ecological geography of the sea*. Cambridge, MA: Academic Press.

Marinov, I., Doney, S. C., & Lima, I. D. (2010). Response of ocean phytoplankton community structure to climate change over the 21st century: Partitioning the effects of nutrients, temperature and light. *Biogeosciences*, *7*(12), 3941–3959. https://doi.org/10.5194/bg-7-3941-2010

Maritorena, S., d'Andon, O. H. F., Mangin, A., & Siegel, D. A. (2010). Merged satellite ocean color data products using a bio-optical model: Characteristics, benefits and issues. *Remote Sensing of Environment*, *114*(8), 1791–1804. https://doi.org/10.1016/j.rse.2010.04.002

Maritorena, S., & Siegel, D. A. (2005). Consistent merging of satellite ocean color data sets using a bio-optical model. *Remote Sensing of Environment*, *94*(4), 429–440. https://doi.org/10.1016/j.rse.2004.08.014

McClain, C. R. (2009). A decade of satellite ocean color observations. *Annual Review of Marine Science*, *1*, 19–42. https://doi.org/10.1146/annurev.marine.010908.163650

Moore, C. M., Mills, M. M., Arrigo, K. R., Berman-Frank, I., Bopp, L., Boyd, P. W., et al. (2013). Processes and patterns of oceanic nutrient limitation. *Nature Geoscience*, *6*, 701–710. https://doi.org/10.1038/ngeo1765

Moses, W. J., Gitelson, A. A., Berdnikov, S., & Povazhnyy, V. (2009). Estimation of chlorophyll-a concentration in case II waters using MODIS and MERIS data-successes and challenges. *Environmental Research Letters*, *4*(4), 045005. https://doi.org/10.1088/1748-9326/4/4/045005

O'Connor, M. I., Piehler, M. F., Leech, D. M., Anton, A., & Bruno, J. F. (2009). Warming and resource availability shift food web structure and metabolism. *PLoS Biology*, *7*(8), e1000178. https://doi.org/10.1371/journal.pbio.1000178

Park, J.-Y., Kug, J.-S., Bader, J., Rolph, R., & Kwon, M. (2015). Amplified Arctic warming by phytoplankton under greenhouse warming. *Proceedings of the National Academy of Sciences of the United States of America*, *112*(19), 5921–5926. https://doi.org/10.1073/pnas.1416884112

Racault, M.-F., Le Quéré, C., Buitenhuis, E., Sathyendranath, S., & Platt, T. (2012). Phytoplankton phenology in the global ocean. *Ecological Indicators*, *14*(1), 152–163. https://doi.org/10.1016/j.ecolind.2011.07.010

Regaudie-De-Gioux, A., & Duarte, C. M. (2012). Temperature dependence of planktonic metabolism in the ocean. *Global Biogeochemical Cycles*, *26*, GB1015. https://doi.org/10.1029/2010GB003907

Roxy, M. K., Modi, A., Murtugudde, R., Valsala, V., Panickal, S., Prasanna Kumar, S., et al. (2016). A reduction in marine primary productivity driven by rapid warming over the tropical Indian Ocean. *Geophysical Research Letters*, *43*, 826–833. https://doi.org/10.1002/2015GL066979

Sherman, E., Moore, J. K., Primeau, F., & Tanouye, D. (2016). Temperature influence on phytoplankton community growth rates. *Global Biogeochemical Cycles*, *30*, 550–559. https://doi.org/10.1002/2015GB005272

Sipelgas, L., Raudsepp, U., & Kõuts, T. (2006). Operational monitoring of suspended matter distribution using MODIS images and numerical modelling. *Advances in Space Research*, *38*(10), 2182–2188. https://doi.org/10.1016/j.asr.2006.03.011

Talmy, D., Blackford, J., Hardman-Mountford, N. J., Dumbrell, A. J., & Geider, R. J. (2013). An optimality model of photoadaptation in contrasting aquatic light regimes. *Limnology and Oceanography*, *58*(5), 1802–1818. https://doi.org/10.4319/lo.2013.58.5.1802

Taucher, J., & Oschlies, A. (2011). Can we predict the direction of marine primary production change under global warming? *Geophysical Research Letters*, *38*, L02603. https://doi.org/10.1029/2010GL045934

Thomas, M. K., Aranguren-Gassis, M., Kremer, C. T., Gould, M. R., Anderson, K., Klausmeier, C. A., & Litchman, E. (2017). Temperature-nutrient interactions exacerbate sensitivity to warming in phytoplankton. *Global Change Biology*, *23*(8), 3269–3280. https://doi.org/10.1111/gcb.13641

Thomas, M. K., Kremer, C. T., Klausmeier, C. A., & Litchman, E. (2012). A global pattern of thermal adaptation in marine phytoplankton. *Science*, *338*(6110), 1085–1088. https://doi.org/10.1126/science.1224836

Toseland, A., Daines, S. J., Clark, J. R., Kirkham, A., Strauss, J., Uhlig, C., et al. (2013). The impact of temperature on marine phytoplankton resource allocation and metabolism. *Nature Climate Change*, *3*(11), 979–984. https://doi.org/10.1038/nclimate1989

Wood, S. N. (2006). *Generalized additive models: An introduction with R*. Chapman &Hall/CRC. https://doi.org/10.1201/9781420010404